

## ORIGINAL ARTICLE

# Versatile inhibition of marine organism settlement by zwitterionic polymer brushes

Yuji Higaki<sup>1,2,3</sup>, Jin Nishida<sup>1</sup>, Ai Takenaka<sup>1</sup>, Rika Yoshimatsu<sup>1</sup>, Motoyasu Kobayashi<sup>1</sup> and Atsushi Takahara<sup>1,2,3</sup>

The anti-fouling character of polymer brushes against marine organisms was investigated by performing settlement tests with barnacle cypris larvae and mussel larvae in their adhesion period, as well as a marine bacteria colonization test. The settlement behavior of the marine organisms was carefully observed during the assays to obtain insight into the anti-fouling character. Zwitterionic poly(phosphobetaine) brushes and poly(sulfobetaine) brushes exhibited excellent anti-fouling characteristics for both macro- and micro-organisms, whereas poly(quaternary ammonium cation) brushes allowed mussel larvae settlement and bacteria adhesion. Regardless of the surface free energy and chain mobility, all of the hydrophobic polymer brushes showed poor anti-fouling character for the marine organisms tested. The surface charge and hydration state in saline seawater appear to be important factors in the versatile anti-fouling performance of zwitterionic polyelectrolyte brushes.

*Polymer Journal* (2015) 47, 811–818; doi:10.1038/pj.2015.77; published online 16 September 2015

## INTRODUCTION

Biofouling is a critical problem in the marine industry.<sup>1,2</sup> Marine organism settlement leads to reductions in the fuel efficiency and navigation performance of ocean vessels, as well as deterioration in the heat exchange capacity of seawater cooling systems in thermal and atomic power plants. More than 4000 marine fouling organisms have been identified and can be categorized as either micro-organisms (for example, bacteria, diatoms and algae spores) or macro-organisms (for example, barnacles, tube worms, mussels and algae). Marine fouling develops in stages, beginning with the formation of an initial conditioning film (adsorption of proteins, polysaccharides and so on) and proceeding to primary colonization (adsorption and growth of bacteria and biofilm formation), secondary colonization (micro-organism settlement and slime formation) and tertiary colonization (macro-organism settlement and growth). Versatile solutions for all fouling stages are desired, but this goal remains elusive due to the wide variety of fouling species and the associated fouling mechanisms. The use of anti-biofouling systems in a marine environment requires extreme durability compared with conventional anti-biofouling systems addressing non-specific adsorption of single-proteins (for example, fibrinogen and bovine serum albumin (BSA)) in moderate ambient conditions. In the marine environment, the diverse organisms, mechanical damage and harsh environmental conditions, which span a broad range of temperatures, salinity and sunlight irradiation, synergistically affect the anti-fouling life. Anti-fouling marine coatings for ship bottom paints have been developed to prevent the undesirable settlement of marine organisms but generally have a significant environmental cost.<sup>2,3</sup> Conventional anti-fouling marine coatings are extremely effective but adversely affect aquatic life

and have led to serious damage to marine environments. International prohibition against toxic anti-fouling coatings has stimulated the development of non-toxic anti-fouling approaches that do not utilize biocide components. Several alternatives to biocidal coatings have been already developed, such as fouling release coatings,<sup>2,4</sup> micro-topographical surfaces<sup>5,6</sup> and self-polishing coatings with a hydrogel-like swollen layer.<sup>7</sup> Fouling release coatings release weakly settled fouling organisms by hydrodynamic shear stress during navigation and generally consist of silicone and/or fluoropolymer-based resins because of their low surface free energy. The fouling release property also depends on other parameters, including the elastic modulus, thickness and surface roughness of the coatings. Microtopographical surfaces are employed by natural marine organisms as a defense against bio-fouling, and numerous artificial biomimetic surfaces have been reported for super-hydrophobic, oleophobic and anti-biofouling applications.<sup>8</sup> While the anti-fouling potential of microtopographical structures has been demonstrated, the underlying mechanism remains unclear. Changes in wettability, surface fluid dynamics and attachment point reduction have been cited as potential factors contributing to the improved anti-fouling performance.

Extensive investigations have focused on the correlation between the organic surface components and the adsorption of micro-organisms and biomacromolecules, particularly proteins, bacteria, cells and marine fouling species.<sup>9–11</sup> Langmuir–Blodgett monolayers, self-assembled monolayers and polymer brushes have been used as model surfaces. Static assays have demonstrated that hydrophobic surfaces tend to promote more non-specific adsorption compared with hydrophilic surfaces. The anti-biofouling character of non-charged hydrophilic polymers has been elucidated and has been

<sup>1</sup>Japan Science and Technology Agency (JST), ERATO Takahara Soft Interfaces Project, Fukuoka, Japan; <sup>2</sup>Institute for Materials Chemistry and Engineering, Kyushu University, Fukuoka, Japan and <sup>3</sup>International Institute for Carbon-Neutral Energy Research (WPI-I2CNER), Kyushu University, Fukuoka, Japan  
Correspondence: Dr Y Higaki or Professor A Takahara, Institute for Materials Chemistry and Engineering, Kyushu University, 744 Motooka, Nishi-ku, Fukuoka 819-0395, Japan.  
E-mail: y-higaki@cstf.kyushu-u.ac.jp or takahara@cstf.kyushu-u.ac.jp

Received 6 July 2015; accepted 27 July 2015; published online 16 September 2015

shown to effectively hinder marine organism settlement. Poly(ethylene glycol) is one of the best synthetic non-fouling polymers, and it exhibits resistance to protein adsorption, cell adhesion, bacterial colonization and marine algae zoospore adsorption.<sup>12–15</sup> The steric exclusion effect, surface hydration and neutral surface potential are generally regarded as key factors in the anti-biofouling performance of poly(ethylene glycol). Zwitterionic polyelectrolytes are promising alternatives to poly(ethylene glycol) for biofouling applications. The anti-fouling efficiency of zwitterionic polyelectrolytes against marine organisms has already demonstrated.<sup>16–22</sup> In particular, poly(phosphobetaine)s have been recognized as bio-inspired anti-biofouling materials, and their neutral surface potential and hydration state are regarded as critical features contributing to the observed bio-inertness.<sup>23–25</sup> Polymer chain grafting is an effective and facile way to modify surface properties without compromising bulk material performance.<sup>17,26,27</sup> Recent developments in surface-initiated controlled radical polymerization procedures have enabled the preparation of so-called high-density ‘polymer brushes,’ which are densely grafted polymer layers without significant defects.<sup>28</sup> The surface-tethered polymer chains swell in good solvents and extend away from the interface to avoid chain overlap. This long-range repulsion between individual chains provides a thick shielding layer at the interface. Zwitterionic polyelectrolyte brushes have been found to exhibit extraordinary super-hydrophilicity and oil-repellency.<sup>29–31</sup> The hydrated polyelectrolyte brushes exhibit low adhesion of foreign objects and outstanding lubrication under wet conditions. While the anti-fouling efficiency of zwitterionic polyelectrolyte brushes for marine organisms has been demonstrated, in many cases the discussion has been limited to the relationship between the number of the settled organisms and the chemical structure of the polymer brushes.<sup>16</sup> The swelling state,<sup>31–35</sup> electrostatic interactions<sup>36</sup> and thickness of the hydrodynamic lubrication layer<sup>37</sup> of polyelectrolyte

brushes have been found to have essential roles in determining the physical properties of polyelectrolyte brushes.

In this paper, the anti-biofouling character of a wide variety of polymer brushes against three marine organisms, a barnacle cypris larva, a mussel larva in its adhesion period and marine bacteria, was investigated by settlement tests and careful observations of the settlement behavior.

## EXPERIMENTAL PROCEDURE

### Preparation of polymer brushes

Polymer brush samples were prepared on a Si wafer substrate through SI-ATRP (surface-initiated atom transfer radical polymerization).<sup>30,38</sup> Si wafers with dimensions of 40 mm length, 10 mm width and 0.5 mm thickness were activated by immersion in piranha solution to remove the oxidized layer and generate hydroxyl groups, after which a silane-coupling reagent with an ATRP-initiating moiety was immobilized on the surface. Polymer brushes were prepared by ATRP in the presence of the initiator-immobilized Si wafer substrate. A variety of polymer brushes were prepared for the settlement tests, including a cationic poly(quaternary ammonium salt) (poly[2-(methacryloyloxy)ethyltrimethylammonium chloride], PMTAC), a zwitterionic poly(phosphobetaine) (poly[2-(methacryloyloxy)ethyl phosphorylcholine], PMPC), zwitterionic poly(sulfobetaine)s (poly(3-[dimethyl(2'-methacryloyloxyethyl)ammonio]ethanesulfonate), PMAES); poly(3-[dimethyl(2'-methacryloyloxyethyl)ammonio]propanesulfonate), PMAPS; poly(3-[dimethyl(2'-methacryloyloxyethyl)ammonio]butanesulfonate), PMABS, hydrocarbon polymers (polystyrene, PS; poly(methyl methacrylate), PMMA; poly(butyl acrylate), PBA), and silicone-containing polymers (poly(3-[tris(trimethylsiloxy)silyl]propylmethacrylate), PTMSM); poly(3-[poly(dimethylsiloxy)silyl]propylmethacrylate), PDMSM (Figure 1). We chose three types of poly(sulfobetaine) brushes because they exhibit different hydrophilicity and swelling, as well as different dependences on temperature and salt concentration. The preparation of PMTAC, PMPC, PMAES, PMAPS, PMABS, PS and PMMA polymer brushes was carried out following previously reported procedures.<sup>30,38</sup> The polymer brush preparation procedures for PTMSM, PDMSM and PBA are described in

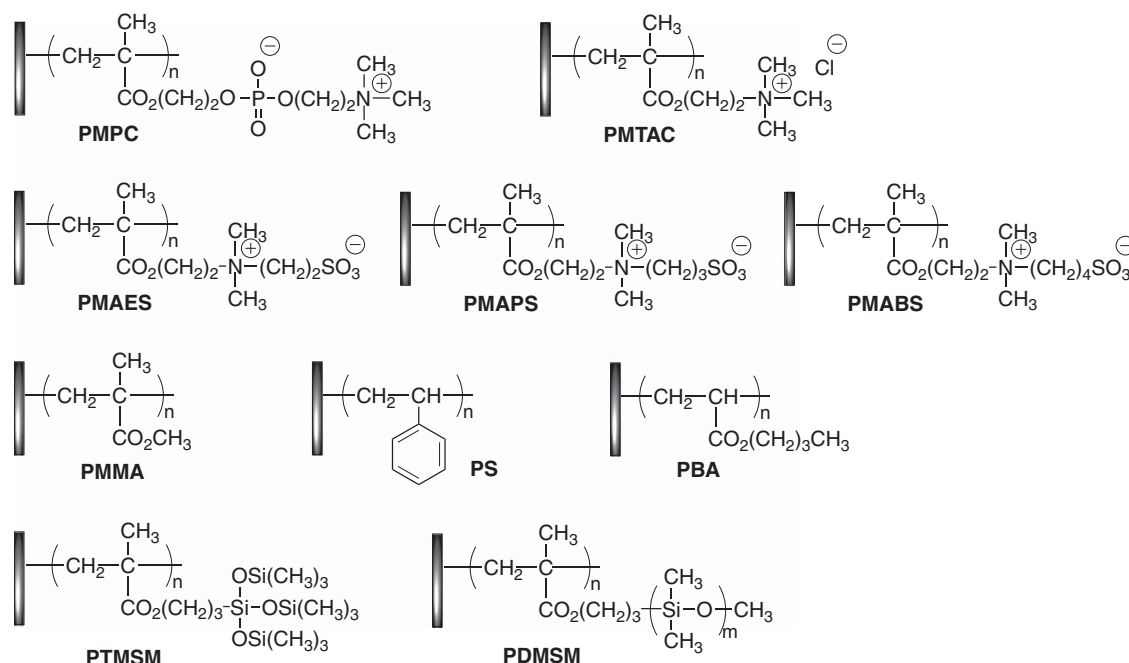


**Figure 1** Chemical structure and abbreviations of the polymer brushes used for marine organism fouling tests. PBA, poly(butyl acrylate); PDMSM, poly(3-[poly(dimethylsiloxy)silyl]propylmethacrylate); PMABS, poly(3-[dimethyl(2'-methacryloyloxyethyl)ammonio]butanesulfonate); PMAES, poly(3-[dimethyl(2'-methacryloyloxyethyl)ammonio]ethanesulfonate); PMAPS, poly(3-[dimethyl(2'-methacryloyloxyethyl)ammonio]propanesulfonate); PMMA, poly(methyl methacrylate); PMPC, poly[2-(methacryloyloxy)ethyl phosphorylcholine]; PMTAC, poly[2-(methacryloyloxy)ethyltrimethylammonium chloride]; PS, polystyrene; PTMSM, poly(3-[tris(trimethylsiloxy)silyl]propylmethacrylate).

Supplementary Information. Because residual copper catalyst has an adverse effect on marine organism settlement, the polymer brush samples were washed carefully using a Soxhlet apparatus to completely remove residual copper.

The number averaged molecular weight ( $M_n$ ) and molecular weight distribution ( $M_w/M_n$ ) were evaluated by size exclusion chromatography with a refractive index detector and a multi-angle light scattering detector. The thicknesses of the polymer brushes were measured by ellipsometry. The surface chemical composition of the polymer brushes was evaluated using X-ray photoelectron spectroscopy. The surface free energy was calculated from the Owens–Wendt equation using static contact angles of water and diiodomethane droplets. Details of the measurement conditions are provided in the Supplementary Information. The chemical structures and characteristics of the polymer brushes used in this paper are summarized in Figure 1 and Table 1. We previously demonstrated that the molecular weights of polymer brushes correspond well to those of free polymers that are grown from the sacrificial initiators.<sup>33,39</sup> The  $M_n$  and  $M_w/M_n$  given in Table 1 are values for free polymers. Graft density was calculated from the  $M_n$  and film thickness.

### Preparation of barnacle cypris larvae

Natural seawater was obtained from the Himeji bay area (Hyogo, Japan) and used after filtration with a 0.45- $\mu$ m mesh cellulose membrane filter (Toyo Roshi Kaisha, Ltd., Tokyo, Japan). Adult barnacles were acquired from the Himeji bay area and stored in plastic 20 l circulation aquaria with aeration at a controlled temperature of 23 °C. The barnacles were fed a daily diet of nauplius larvae of the brine shrimp *Artemia salina*. After being hatched from the adults, the nauplius larvae were collected using a pipette and transferred to a glass beaker with filtered natural seawater. The larvae were fed with the diatom *Cheateoceros calcitrans* to cultivate cypris larvae. The nauplius larvae were stored at 23 °C, and the cypris larvae of *Amphibalanus amphitrite* were obtained by metamorphosis. The cypris larvae were kept under cold (6 °C) and dark conditions until the bioassay. The temperature of the seawater was restored to room temperature (23 °C) before the settlement test. A light source was provided to select photopositive and actively swimming individuals, and the active individuals were collected and used for the settlement assay.

### Preparation of mussel larvae

Natural seawater was collected from the Himeji bay area and used after filtration through a 0.45- $\mu$ m mesh cellulose membrane filter (Toyo Roshi Kaisha, Ltd.). Adult blue mussels were obtained from Kakogawa (Hyogo, Japan) and maintained in plastic 20 l aquaria. Fertilized eggs of the mussels

were obtained by stimulating mussel fertilization and were subsequently washed and transferred to a glass beaker. D-type larvae were cultured in filtered seawater by feeding with diatom plankton (*Haptophyceae isochrysis*). A mixture of streptomycin and penicillin was added to the beaker to prevent bacterial growth. After culturing for 45 days, mussel larvae with an average shell length of 0.7 mm were obtained. The mussel larvae were kept at 6 °C in the dark in filtered seawater. Active larvae that readily adhered by creeping were collected and used for the settlement assay.

### Barnacle cypris larvae settlement test

A polystyrene container (Highpack S-9) with dimensions of 84 mm length  $\times$  57 mm width  $\times$  44 mm depth was covered with a plankton filtering net to avoid barnacle cypris larvae settlement onto the container wall. Natural filtered seawater (50 ml), 2 pieces of the same type of polymer brush and 40 artificially grown barnacle cypris larvae were added to the container. Settlement tests were carried out in discrete containers for each polymer brush species (that is, the tests were not ‘choice assays’ in which several types of substrates are introduced into the container). The temperature was maintained at 25 °C, and the container was placed on a lighting table to encourage the photoactive cypris larvae to approach the test pieces. The cypris larvae trapped at the water surface were circulated by applying water droplets once every day. Cypris larvae that actively walked along the substrates with antennule attachment were termed as ‘searching,’ whereas those in the primary settlement stage and that had metamorphosed into juveniles were designated as ‘settled’ in this study. The numbers of ‘searching’ and ‘settled’ cypris larvae were counted daily using an optical microscope. Because only a single settlement test was performed for each polymer brush, statistical analysis was not conducted and the data are provided as the ratio of settled cypris larva to the initial population without error bars. The condition of the cypris larvae was carefully observed and monitored with photographs and movies to gain insight on settlement inhibition.

### Mussel larvae settlement test

Natural filtered seawater (15 ml) and two pieces of the same type of polymer brush were added to a plastic container (30 ml volume) and maintained at 25 °C. Twenty-five active mussel larvae in their adhesion period were placed on the polymer brush samples, and the numbers of mussel larvae that were ‘searching’ and ‘settled’ on the substrates were counted daily using an optical microscope. The tests lasted for 6 days and the anti-settlement efficiency was evaluated based on the ratio of ‘settled’ mussel larvae to the initial population after the settlement test period. Because the only one settlement test was performed for each polymer brush, statistical analysis was not performed and the data are provided without error bars.

### Marine bacteria colonization test

Natural seawater was acquired from Himeji bay area and filtered using a 5.0- $\mu$ m mesh cellulose membrane filter (Toyo Roshi Kaisha, Ltd., qualitative filter paper No. 2) to remove large objects. The bacteria species and populations in the natural seawater were not identified, but all the tests were carried out simultaneously using the same seawater source. The water quality of the filtered seawater was 29.0 psu and pH 7.90. Filtered seawater (15 ml) and two pieces of the same type of polymer brush were added into a polystyrene container (Highpack S-9) with dimensions of 84 mm length  $\times$  57 mm width  $\times$  44 mm depth. After 6 days of immersion, a formalin solution was introduced (3% concentration) to fix the bacteria on the substrate. The test pieces were subsequently removed from the vessel and then immersed in a filtered and sterilized tris-buffer solution. A 50  $\mu$ g ml<sup>-1</sup> 4',6-diamidino-2-phenylindole solution was added to the solution to stain the bacteria for subsequent observation. The stained bacteria were visualized by fluorescence microscopy (Olympus Corporation, Tokyo, Japan, BX51-WU, excitation wave length: 330–384 nm), and the number of bacteria in the field was counted. For each sample, 10 images were taken to obtain an average number of bacteria adhered to the surface, and the average number and the standard deviation were calculated.

**Table 1** Characteristics of polymer brush samples

	$M_n^a$	$M_w/M_n^a$	Thickness <sup>b</sup> (nm)	Graft density <sup>c</sup> (chains per nm <sup>2</sup> )
PMPC	349 000	1.56	85	0.20
PMAES	733 000	1.22	173	0.19
PMAPS	326 000	1.20	105	0.26
PMABS	180 000	1.85	115	0.52
PMTAC	269 000	1.14	110	0.33
PMMA	169 000	1.16	104	0.44
PS	401 000	1.87	180	0.28
PBA	98 400	1.57	49	0.30
PTMSM	297 000	3.10	96	— <sup>d</sup>
PDMSM	207 000	1.25	47	0.14

Abbreviations: MALS, multi-angle light scattering; PBA, poly(butyl acrylate); PDMSM, poly(3-[poly(dimethylsiloxy)silyl]propylmethacrylate); PMABS, poly(3-[dimethyl(2'-methacryloyloxyethyl) ammonio]butanesulfonate); PMAES, poly(3-[dimethyl(2'-methacryloyloxyethyl)ammonio]ethanesulfonate); PMAPS, poly(3-[dimethyl(2'-methacryloyloxyethyl)ammonio]propanesulfonate); PMMA, poly(methyl methacrylate); PMPC, poly(2-(methacryloyloxy)ethyl phosphorylcholine); PMTAC, poly(2-(methacryloyloxy)ethyltrimethylammonium chloride); PS, polystyrene; PTMSM, poly(3-[tris(trimethylsiloxy)silyl]propylmethacrylate); RI, refractive index; SEC, size exclusion chromatography.

<sup>a</sup> $M_n$  and  $M_w/M_n$  determined by SEC equipped with a RI detector and MALS detector.

<sup>b</sup>Thickness in dry state ( $L$ ) estimated by ellipsometry.

<sup>c</sup>Graft density,  $\sigma$ , calculated from determined values of  $M_n$  and  $L$  using equation  $\sigma = \rho L N_A / M_n$ , where  $\rho$  is the bulk density of the free (unbound) polymer and  $N_A$  is Avogadro's constant.

<sup>d</sup>The graft density calculation was not reliable due to the broad polydispersity index of grafted chains.

## RESULTS AND DISCUSSION

### Preparation of polymer brushes

All of the polymer brush samples had a high graft density ( $>0.1$  chains per  $\text{nm}^2$ ) with respect to conventional dilute polymer brushes prepared by chemical reactions or the interaction of polymer chain-ends with an activated substrate. The thicknesses were above the radius of gyration of an unperturbed random coil, indicating that the lateral osmotic pressure in the tethered polymer chains made the chains adopt a stretched conformation. We assumed that the thickness ( $>50$  nm) was sufficient and that the effects of differences in thickness between the polymer brush samples were not significant for the marine organism settlement tests; the thickness range was far beyond the interaction field of the substrate. The surface chemical compositions obtained from the X-ray photoelectron spectroscopy spectra were consistent with the chemical compositions of the grafted polymer chains. The silicon peak disappeared after polymer brush grafting, indicating that the silicon wafer was covered with a thick polymer brush layer with thickness greater than the mean free path of the photoelectron ( $\sim 10$  nm) without significant defects. The bulk glass transition temperatures ( $T_g$ ), contact angles for water and diiodomethane droplets and calculated surface free energies of the polymer brush samples are summarized in Table 2. It should be noted that the surface free energies calculated from the Owens–Wendt equation are not reliable, especially for hydrophilic surfaces because the polymer chains penetrate the probing liquid and reduce the interfacial tension. A clear glass transition was not observed below 473 K for the cationic and zwitterionic polymers due to their strong electrostatic interactions. For hydrophobic polymers, the bulk  $T_g$  can be regarded as a reference for thermal molecular motion of the polymer brushes at the seawater interface. The charged polyelectrolyte brushes showed characteristic swelling, depending on the temperature and salt concentration.<sup>34</sup> In the swollen state, the polymer brushes

exhibited a greater number of possible conformations, owing to the strong hydration, which help prevent the adhesion of foreign bodies. Each of the cationic and zwitterionic polyelectrolyte brushes exhibited high surface free energy, whereas the hydrocarbon polymers and silicone-containing polymers had low surface free energy.

### Barnacle cypris larvae settlement test

Barnacles start life as nauplius larvae that feed on plankton, and the final larval stage is the cypris larva, which is approximately 500  $\mu\text{m}$  in length and does not feed but rather swims in water. To complete the transition to adult life, cypris larvae need to attach temporarily to a hard substrate. During this exploration phase, the cypris larvae explore suitable sites for attachment by ‘walking’ on substrates using a pair of attachment apparatuses at their antennule tips that secrete an adhesive substance.<sup>39,40</sup> The antennal tip repeatedly attaches and detaches from the substrate. Their temporary repeatable adhesion has been explained by van der Waals interactions during the contact of splitting cuticular villi at the antennular disk and capillary adhesion of non-polar viscous glycoproteins at the antennular secretion. After the exploration stage, the cypris larvae remain on a suitable site and metamorphose into juveniles. The firmly attached juvenile subsequently metamorphoses into a calcified adult barnacle that strongly adheres to the substrate by secreting cementing proteins.<sup>41</sup>

The evolution of the number of ‘settled’ cypris larvae on the polymer brushes is shown in Figure 2. On the bare Si wafer and hydrophobic polymer brushes, enthusiastic searching was observed (Supplementary Movie S1). For the bare Si wafer, 63% of the cypris larvae settled after 10 days of immersion. In contrast, the cypris larvae showed no searching activity on the cationic and zwitterionic polyelectrolyte brushes throughout the test period (10 days) (Supplementary Movie S2). The cypris larvae were positioned sideways on the cationic and zwitterionic polymer brushes rather than face-on, as observed on the bare Si wafer and hydrophobic polymer brushes, and cypris larvae walking with antennule apparatus attachment were rarely observed. All the introduced cypris larvae showed active exploration at the plankton filtering net, indicating that the artificially cultured cypris larvae had a high settlement ability. To confirm activity of the cypris larvae during the test period, bare Si wafers were placed in the test containers after the settlement tests. Most of the remaining unsettled cypris larvae immediately settled on the Si wafers within a day. Because we selected photopositive and actively swimming individuals for the settlement assay, they remained active even after the 10-day test period, while the weak cypris larvae are usually starved to death in short periods. It is apparent that the excellent anti-settlement performance of the hydrophilic charged polymer brushes is related to inhibition of the ‘walking’ and ‘searching’ activities of the barnacle cypris larvae, whereas the hydrophobic polymer brushes did not appear to discourage exploration.<sup>42</sup> The exploration inhibition observed may be related to the low adhesion of antennule tips resulting from the lubricating effects of the hydrated polyelectrolyte brushes.

### Mussel larvae settlement test

The marine mussel successfully inhabits niches in intertidal zones using a byssus to glue itself to a wide variety of substrates. The byssus consists of a bundle of collagenous threads tipped with an adhesive plaque. The mussel adhesive plaque proteins have been identified and are referred to as mussel foot proteins (m.f.p.).<sup>43–45</sup> Amino acids with post-translationally modified side chains are present in large quantities in the m.f.p., and the proteins include a significant number of basic residues. The secretion contains micromolar concentrations of  $\text{Fe}^{3+}$

**Table 2** Glass transition temperature, contact angles and surface free energy of polymer brushes

	$T_g^a$ (K)	Static contact angles <sup>b</sup> (deg)		$\gamma_{\text{SV}}^c$	$\gamma_{\text{SV}}^{d,c}$	$\gamma_{\text{SV}}^{p,c}$
				( $\text{mJ m}^{-2}$ )	( $\text{mJ m}^{-2}$ )	( $\text{mJ m}^{-2}$ )
		Water	Diiodomethane			
PMPc	—	$< 3$	$27 \pm 1.9$	74.5	33.5	41.0
PMAES	—	$14 \pm 4.1$	$38 \pm 1.5$	71.6	29.2	42.4
PMApS	—	$15 \pm 2.4$	$33 \pm 2.4$	71.8	31.5	40.4
PMAbS	—	$52 \pm 3.8$	$48 \pm 2.4$	50.6	27.5	23.1
PMTAc	—	$10 \pm 3.0$	$45 \pm 0.9$	72.0	25.6	46.5
PMMA	378	$75 \pm 2.6$	$36 \pm 1.4$	43.5	37.7	5.8
PS	370	$89 \pm 3.1$	$37 \pm 0.8$	41.1	40.0	1.1
PBA	224	$91 \pm 0.7$	$57 \pm 1.9$	30.7	28.4	2.3
PTMSM	276	$107 \pm 4.5$	$75 \pm 2.6$	20.1	19.6	0.5
PDMSM	136	$106 \pm 0.6$	$85 \pm 2.4$	15.4	13.8	1.6

Abbreviations: PBA, poly(butyl acrylate); PDMSM, poly(3-[poly(dimethylsiloxy)silyl]propylmethacrylate); PMAbS, poly(3-[dimethyl(2'-methacryloyloxyethyl)ammonio]butanesulfonate); PMAES, poly(3-[dimethyl(2'-methacryloyloxyethyl)ammonio]ethanesulfonate); PMApS, poly(3-[dimethyl(2'-methacryloyloxyethyl)ammonio]propanesulfonate); PMMA, poly(methyl methacrylate); PMPc, poly[2-(methacryloyloxy)ethyl phosphorylcholine]; PMTAc, poly[2-(methacryloyloxy)ethyltrimethylammonium chloride]; PS, polystyrene; PTMSM, poly(3-[tris(trimethylsiloxy)silyl]propylmethacrylate).

<sup>a</sup>Glass transition temperature ( $T_g$ ) of the bulk polymers determined by differential scanning calorimetry (DSC) measurement. The heating and cooling rate was 10 K per minute.

<sup>b</sup>All static contact angles were measured with 2  $\mu\text{l}$  droplet.

<sup>c</sup> $\gamma_{\text{SV}}^d$  and  $\gamma_{\text{SV}}^p$  are the dispersion and polar force components of the solid-vapor interface free energy, respectively, and were determined from contact angles of water and diiodomethane droplets by the Owens–Wendt method using the following parameters:  $\gamma_{\text{LV}}^d$  (water) = 21.8,  $\gamma_{\text{LV}}^p$  (water) = 51.0,  $\gamma_{\text{LV}}^d$  (diiodomethane) = 49.5,  $\gamma_{\text{LV}}^p$  (diiodomethane) = 1.3  $\text{mJ m}^{-2}$ .



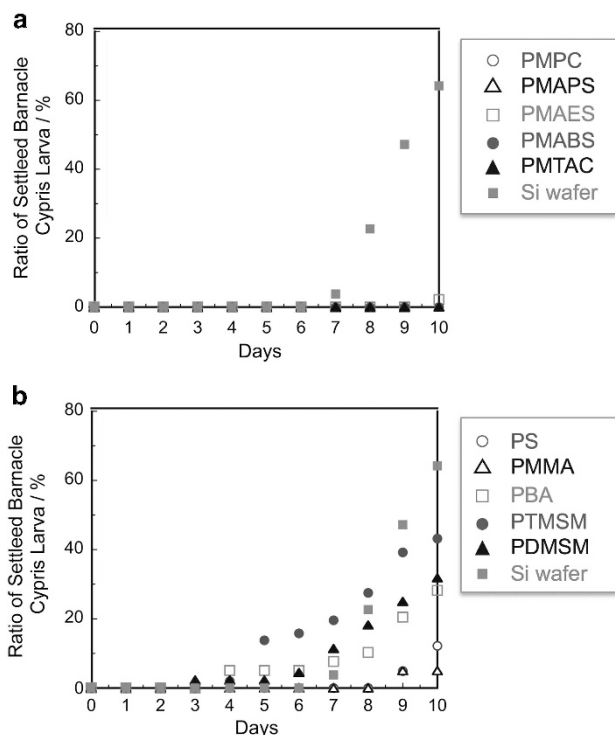


**Figure 2** Evolution of the ratio of 'settled' barnacle cypris larva on (a) zwitterionic and cationic polyelectrolyte brushes and (b) hydrocarbon and silicone-containing polymer brushes during the settlement tests. PBA, poly(butyl acrylate); PDMSM, poly(3-[poly(dimethylsiloxy)silyl]propylmethacrylate); PMABS, poly(3-[dimethyl(2'-methacryloyloxyethyl)ammonio]butanesulfonate); PMAES, poly(3-[dimethyl(2'-methacryloyloxyethyl)ammonio]ethanesulfonate); PMAPS, poly(3-[dimethyl(2'-methacryloyloxyethyl)ammonio]propanesulfonate); PMMA, poly(methyl methacrylate); PMPC, poly[2-(methacryloyloxy)ethyl phosphorylcholine]; PMTAC, poly[2-(methacryloyloxy)ethyltrimethylammonium chloride]; PS, polystyrene; PTMSM, poly(3-[tris(trimethylsiloxy)silyl]propylmethacrylate). A full color version of this figure is available at *Polymer Journal* online.

ions to assist with curing. The rapid adhesion and high adhesive strength of the byssus plaque has drawn considerable attention as a model system for adhesives that are effective in wet conditions.<sup>46–48</sup> The attachment process of a mussel using byssus threads resembles reaction injection molding and consists of three major steps: (a) exploration and identification of a suitable site for settlement by 'walking' via temporary attachment of the suction pad at the byssus tip, (b) pressing the suction pad to the substrate to remove water in the cavity and (c) secreting m.f.p. into the cavity of the suction pad to adhere the byssus to the substrate.

Settlement of the mussel larvae was evaluated by counting the number of settled mussel larvae after the 6-day test period (Figure 3). The zwitterionic polyelectrolytes (PMPC, PMAES, PMAPS and PMABS) showed the most significant inhibition of mussel larvae settlement, followed by more modest inhibition by the cationic polyelectrolyte (PMTAC) and negligible effects for the hydrophobic polymers (PS, PMMA, PTMSM and PDMSM) relative to a bare Si wafer. Similar to the barnacle cypris larvae, the zwitterionic polyelectrolyte brushes showed excellent anti-settlement efficiency for mussel larvae. However, unlike the barnacles, the cationic polyelectrolyte brushes permitted settlement of mussel larvae. The mussel larvae settled on the hydrophobic polymer brushes to a similar

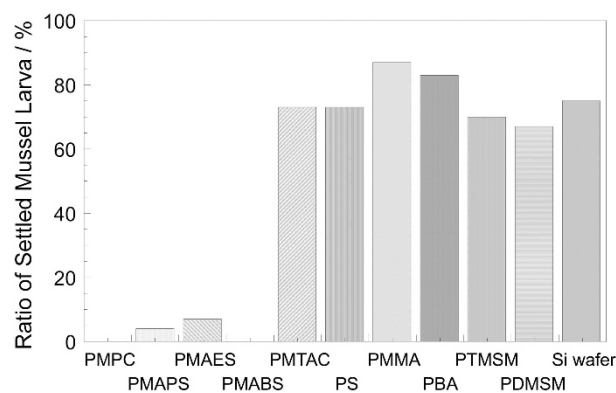


**Figure 3** The ratio of 'settled' mussel larva to the initial population of mussel larva. The number of 'settled' mussel larvae on the polymer brushes was counted after a settlement test period of 6 days. PBA, poly(butyl acrylate); PDMSM, poly(3-[poly(dimethylsiloxy)silyl]propylmethacrylate); PMABS, poly(3-[dimethyl(2'-methacryloyloxyethyl)ammonio]butanesulfonate); PMAES, poly(3-[dimethyl(2'-methacryloyloxyethyl)ammonio]ethanesulfonate); PMAPS, poly(3-[dimethyl(2'-methacryloyloxyethyl)ammonio]propanesulfonate); PMMA, poly(methyl methacrylate); PMPC, poly[2-(methacryloyloxy)ethyl phosphorylcholine]; PMTAC, poly[2-(methacryloyloxy)ethyltrimethylammonium chloride]; PS, polystyrene; PTMSM, poly(3-[tris(trimethylsiloxy)silyl]propylmethacrylate).

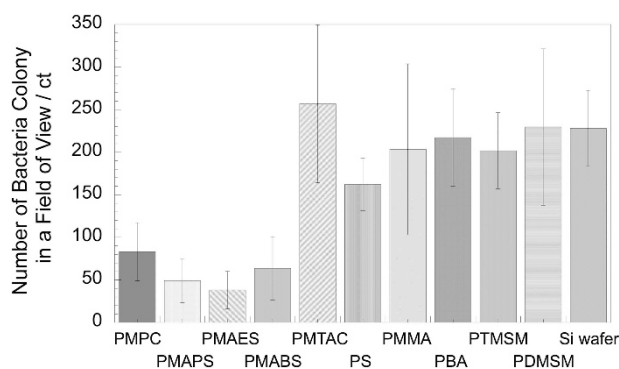


**Figure 4** Number of bacteria on the polymer brushes in microscopic fields. The data were averaged from 10 observations. Error bars represent the s.d. PBA, poly(butyl acrylate); PDMSM, poly(3-[poly(dimethylsiloxy)silyl]propylmethacrylate); PMABS, poly(3-[dimethyl(2'-methacryloyloxyethyl)ammonio]butanesulfonate); PMAES, poly(3-[dimethyl(2'-methacryloyloxyethyl)ammonio]ethanesulfonate); PMAPS, poly(3-[dimethyl(2'-methacryloyloxyethyl)ammonio]propanesulfonate); PMMA, poly(methyl methacrylate); PMPC, poly[2-(methacryloyloxy)ethyl phosphorylcholine]; PMTAC, poly[2-(methacryloyloxy)ethyltrimethylammonium chloride]; PS, polystyrene; PTMSM, poly(3-[tris(trimethylsiloxy)silyl]propylmethacrylate).

degree as the bare Si wafers, and no significant dependence on the chemical structure was observed.

In contrast to the barnacle cypris larvae, the mussel larvae showed active exploration on all of the polymer brushes, including the zwitterionic polyelectrolyte brushes (Supplementary Movie 3, play time: 8–15 s). The larvae crept on the polymer brush surfaces by attaching their feet. However, settlement by the byssus adhesion failed (Supplementary Movie 3, play time: 17–19 s). Radially distributed byssuses were observed around the larva, which indicated that the mussel larva attempted to settle on the zwitterionic polyelectrolyte brush surfaces. The larva got into the position by using their foot attachments (Supplementary Movie 3, play time: 53 s), retrieved

settlement and failed again (Supplementary Movie 3, play time: 62 s). The failed attachment was attributed to the low adhesion force between the plaque and polymer brushes. This result was surprising because the m.f.p. is known to be a versatile substrate-independent adhesive. The poor adhesion was attributed to the weak interaction between charged residues and hydroxylated tyrosine (Dopa, 3,4-dihydroxyphenyl-L-alanine) residues with the hydrated poly(zwitterion)s. The zwitterionic polyelectrolyte brushes may be able to retain hydrated water during the vacuum and dewetting processes of byssus adhesion. We previously reported on the swelling of polyelectrolyte brushes, which was analyzed using small angle X-ray scattering and neutron reflectivity.<sup>32,33</sup> PMPC swells both in pure water and in aqueous sodium chloride solutions. Poly(sulfobetaine)s collapse in pure water but swell in aqueous sodium chloride solutions because of the screening effect of electrostatic attractions between the sulfobetaine units. In contrast, PMTAC swells in pure water but collapses in aqueous sodium chloride solutions because of the screening effect of electrostatic repulsion between quaternary ammonium cations. The adhesion force of m.f.p. can be correlated with the volume fraction of the polymer component at the interface, and the electrostatic adhesion will be greatly diminished in the presence of media with a high dielectric constant. Therefore, the PMPC and poly(sulfobetaine)s, which are strongly hydrated in saline

seawater, were able to prevent mussel larvae settlement, whereas the PMTAC, which collapses in a saline environment, permitted m.f.p. adhesion. The hydration state in saline seawater is a more important factor than the hydrophilicity of the polymer brush, because the hydrophilic PMTAC allowed mussel larvae settlement while the PMABS brushes exhibited efficient anti-settlement for mussel larvae. In addition, for the zwitterionic betaine moiety, the hydrogen bonding network structure of the hydrated water was not disrupted due to the neutral charge, which permitted the formation of a stable hydrated layer.<sup>49</sup> The naturally hydrated water in the zwitterionic polyelectrolyte brushes remained at the cavity of the suction pad and thereby reduced the adhesive efficiency of the m.f.p. plaques.

#### Marine bacteria settlement assay for polymer brushes

Marine bacteria are a major constituent in the formation of bio-films. Controlling marine bacteria adhesion is critical for inhibiting slime growth and subsequent macro-fouling settlement. Bacterial adhesion has been treated with Derjaguin-Landau-Verwey-Overbeek (DLVO) theory because the size scale is similar to colloids.<sup>50</sup> Generally, bacteria have a negative charge in basic aqueous solutions due to the dissociation of carboxylic acid and phosphate residues exposed on their surfaces. Marine bacteria approach substrates by Brownian motion and adhere to surfaces weakly by van der Waals

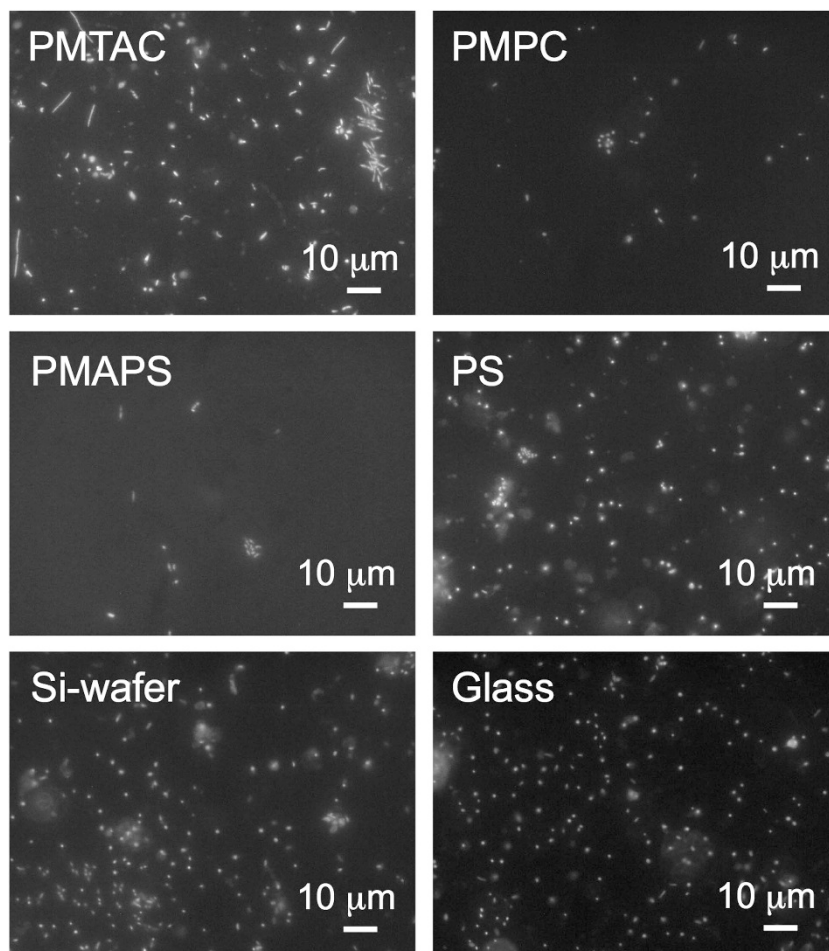


**Figure 5** Fluorescence microscopy images of stained marine bacteria colonies attached to the polymer brushes, silicon wafer and glass substrates after the 6-day test period. PMAPS, poly(3-[dimethyl(2'-methacryloyloxyethyl)ammonio]propanesulfonate); PMPC, poly[2-(methacryloyloxy)ethyl phosphorylcholine]; PMTAC, poly[2-(methacryloyloxy)ethyltrimethylammonium chloride]. A full color version of this figure is available at *Polymer Journal* online.

interaction.<sup>51</sup> Adhesion is achieved by an extracellular polymeric substance, which mainly consists of polysaccharides, penetrating an electric bilayer energy barrier at the interface between the bacteria and the surface.<sup>52</sup> In saline seawater, the electric bilayer is thin and the electrostatic repulsive forces are less effective. In the case of soft colloids with dangling polymer chains on the surfaces (marine bacteria have polysaccharide chains on their outer surfaces), the electrostatic energy barrier is quite low,<sup>52,53</sup> which permits non-specific adhesion of marine bacteria to any substrate, regardless of the surface potential.

The anti-bacteria adsorption efficiency of the polymer brushes was examined by exposing the polymer brush test pieces to natural seawater containing native bacteria (Figures 4 and 5). The efficiency at reducing bacterial colonization was as follows: zwitterionic polyelectrolytes (PMPC, PMAES, PMAPS, PMABS) > hydrophobic polymers (PS, PMMA, PTMSM, PDMSM), unmodified Si wafer > cationic polyelectrolyte (PMTAC). Although the population of bacteria colonies was less for zwitterionic polyelectrolyte brushes than other polymer brushes, a moderate amount of bacteria settlement was observed. Bacteria adhesion to zwitterionic polyelectrolyte brushes was previously reported by Cheng *et al.*<sup>19</sup> They reported that PMAPS brushes showed nearly complete inhibition of bacterial adhesion. However, their test was carried out in the presence of a laminar flow field. The low bacteria colony population on zwitterionic polyelectrolyte brushes was likely due to the detachment of the grown bacteria colonies by shear force during testing. Bacteria colonies adhere weakly on non-charged hydrated zwitterionic polyelectrolyte brushes and are easily detached by water flow. Hydrated water diminishes the electrostatic interactions, and the penetration of water into the bacteria colony/hydrated polyelectrolyte brush interface facilitates colony detachment. The cationic polymer brushes showed a large amount of bacterial adhesion, even after washing. The strong adhesion could also be attributed to the hydration state in saline seawater, as the PMTAC brushes collapsed in saline water to give a non-hydrated positively charged interface. Adhesion protection by the hydration shell and water penetration effects were lost in the saline seawater for the PMTAC brushes. Electrostatic attractions between the ammonium cations and negatively charged bacteria also led to the large amount of bacteria adhesion. Moreover, quaternary ammonium cations are known as a conventional germicide and algicide, and the poly(ammonium cation)s show antibacterial property. Biofilm formation by dead bacteria or microorganisms is thought to lead to bacteria colony adhesion.

## CONCLUSIONS

The zwitterionic polyelectrolyte brushes exhibited versatile anti-fouling character for the marine organisms examined. The poly(quaternary ammonium cation) brushes permitted mussel larvae settlement and bacteria colonization, whereas barnacle cypris larvae settlement was prevented. All of the hydrophobic polymer brushes allowed extreme macro-organism settlement and bacterial colonization. For barnacle cypris larvae, exploration was prevented on the polyelectrolyte brushes due to the weak adhesion force of the antennules to the hydrophilic polymer brush surface. For mussel larvae, the zwitterionic polyelectrolyte brushes permitted exploration but prevented m.f.p. adhesion. The m.f.p. were able to adhere to the poly(quaternary ammonium cation) to a similar degree as was observed for the hydrophobic polymers. The marine bacteria colonies weakly adhered to the zwitterionic polyelectrolyte brushes, leading to facile removal of grown bacterial colonies by shear force. In contrast, the bacteria strongly adhered to the poly(quaternary ammonium cation) brushes. The results demonstrate that zwitterionic

polyelectrolyte brushes show a balanced universal anti-fouling nature, and insight on effective anti-fouling strategies was provided by careful observations of the settlement behavior.

## CONFLICT OF INTEREST

The authors declare no conflict of interest.

## ACKNOWLEDGEMENTS

We are grateful to Dr Kamiya (Sessile Research Corp.) for assistance with the marine organism settlement tests and helpful discussions. We appreciate Dr Kevin L. White's assistance with English editing. This research was partially supported by the Adaptable and Seamless Technology Transfer Program through Target-driven R&D (No. AS2511206M), Japan Science and Technology Agency, JST.

- 1 Yebra, D. M., Kiil, S. & Dam-Johansen, K. Antifouling technology-past, present and future steps towards efficient and environmentally friendly antifouling coatings. *Prog. Org. Coat.* **50**, 75–104 (2004).
- 2 Lejars, M., Margailan, A. & Bressy, C. Fouling release coatings: A nontoxic alternative to biocidal antifouling coatings. *Chem. Rev.* **112**, 4347–4390 (2012).
- 3 Callow, J. A. & Callow, M. E. Trends in the development of environmentally friendly fouling-resistant marine coatings. *Nat. Commun.* **2**, 244–254 (2011).
- 4 Brady, R. F. A fracture mechanical analysis of fouling release from nontoxic antifouling coatings. *Prog. Org. Coat.* **43**, 188–192 (2001).
- 5 Schumacher, J. F., Carman, M. L., Estes, T. G., Feinberg, A. W., Wilson, L. H., Callow, M. E., Callow, J. A., Finlay, J. A. & Brennan, A. B. Engineered antifouling microtopographies – effect of feature size, geometry, and roughness on settlement of zoospores of the green alga *Ulva*. *Biofouling* **23**, 55–62 (2007).
- 6 Liu, X., Zhou, J., Xue, Z., Gao, J., Meng, J., Wang, S. & Jiang, L. Clam's shell inspired high-energy inorganic coatings with underwater low adhesive superoleophobicity. *Adv. Mater.* **24**, 3401–3405 (2012).
- 7 Xie, L., Hong, F., He, C., Ma, C., Liu, J., Zhang, G. & Wu, C. Coatings with a self-generating hydrogel surface for antifouling. *Polymer* **52**, 3738–3744 (2011).
- 8 Bhushan, B. Bioinspired structured surfaces. *Langmuir* **28**, 1698–1714 (2012).
- 9 Chen, S., Zheng, J., Li, L. & Jiang, S. Strong resistance of phosphorylcholine self-assembled monolayers to protein adsorption: Insights into nonfouling properties of zwitterionic materials. *J. Am. Chem. Soc.* **127**, 14473–14478 (2005).
- 10 Ohkubo, Y., Kusu, K., Onishi, S. & Ogawa, K. The anti-biofouling effect against barnacles of a super-hydrophilic and high-oleophobic surface of treated aluminium. *Sessile Organism* **29**, 41–48 (2012).
- 11 Ostuni, E., Chapman, R. G., Liang, M. N., Meluleni, G., Pier, G., Ingber, D. E. & Whitesides, G. M. Self-assembled monolayers that resist the adsorption of proteins and the adhesion of bacterial and mammalian cells. *Langmuir* **17**, 6336–6343 (2001).
- 12 Jeon, S. I., Lee, J. H., Andrade, J. D. & Degennes, P. G. Protein surface interactions in the presence of polyethylene oxide. 1. simplified theory. *J. Colloid Interface Sci.* **142**, 149–158 (1991).
- 13 Hester, J. F., Banerjee, P. & Mayes, A. M. Preparation of protein-resistant surfaces on poly(vinylidene fluoride) membranes via surface segregation. *Macromolecules* **32**, 1643–1650 (1999).
- 14 Wagner, V. E., Koberstein, J. T. & Bryers, J. D. Protein and bacterial fouling characteristics of peptide and antibody decorated surfaces of PEG-poly(acrylic acid) co-polymers. *Biomaterials* **25**, 2247–2263 (2004).
- 15 Schilp, S., Rosenhahn, A., Pettitt, M. E., Bowen, J., Callow, M. E., Callow, J. A. & Grunze, M. Physicochemical properties of (ethylene glycol)-containing self-assembled monolayers relevant for protein and algal cell resistance. *Langmuir* **25**, 10077–10082 (2009).
- 16 Jiang, S. & Cao, Z. Ultralow-fouling, functionalizable, and hydrolyzable zwitterionic materials and their derivatives for biological applications. *Adv. Mater.* **22**, 920–932 (2010).
- 17 Yang, W. J., Neoh, K.-G., Kang, E.-T., Teo, S. L.-M. & Rittschof, D. Polymer brush coatings for combating marine biofouling. *Prog. Polym. Sci.* **39**, 1017–1042 (2014).
- 18 Zhang, Z., Chen, S., Chang, Y. & Jiang, S. Surface grafted sulfobetaine polymers via atom transfer radical polymerization as superlow fouling coatings. *J. Phys. Chem. B* **110**, 10799–10804 (2006).
- 19 Cheng, G., Zhang, Z., Chen, S., Bryers, J. D. & Jiang, S. Inhibition of bacterial adhesion and biofilm formation on zwitterionic surfaces. *Biomaterials* **28**, 4192–4199 (2007).
- 20 Zhang, Z., Finlay, J. A., Wang, L., Gao, Y., Callow, J. A., Callow, M. E. & Jiang, S. Polysulfobetaine-grafted surfaces as environmentally benign ultralow fouling marine coatings. *Langmuir* **25**, 13516–13521 (2009).
- 21 Aldred, N., Li, G., Gao, Y., Clare, A. S. & Jiang, S. Modulation of barnacle (*Balanus amphitrite* Darwin) cypris settlement behavior by sulfobetaine and carboxybetaine methacrylate polymer coatings. *Biofouling* **26**, 673–683 (2010).
- 22 Kitano, H., Kondo, T., Kamada, T., Iwanaga, S., Nakamura, M. & Ohno, K. Anti-biofouling properties of an amphoteric polymer brush constructed on a glass substrate. *Colloids Surf B Biointerfaces* **88**, 455–462 (2011).

- 23 Ishihara, K., Nomura, H., Mihara, T., Kurita, K., Iwasaki, Y. & Nakabayashi, N. Why do phospholipid polymers reduce protein adsorption? *J. Biomed. Mater. Res.* **39**, 323–330 (1998).
- 24 Feng, W., Zhu, S., Ishihara, K. & Brash, J. L. Adsorption of fibrinogen and lysozyme on silicon grafted with poly(2-methacryloyloxyethyl phosphorylcholine) via surface-initiated atom transfer radical polymerization. *Langmuir* **21**, 5980–5987 (2005).
- 25 Iwata, R., Suk-In, P., Hoven, V. P., Takahara, A., Akiyoshi, K. & Iwasaki, Y. Control of nanobiointerfaces generated from well-defined biomimetic polymer brushes for protein and cell manipulations. *Biomacromolecules* **5**, 2308–2314 (2004).
- 26 Zhao, B. & Brittain, W. J. Polymer brushes: surface-immobilized macromolecules. *Prog. Polym. Sci.* **25**, 677–710 (2000).
- 27 Quintana, R., Jariczewski, D., Vasantha, V. A., Jana, S., Lee, S. S. C., Parra-Velandia, F. J., Guo, S., Parthiban, A., Teo, S. L.-M. & Vancso, G. J. Sulfobetaine-based polymer brushes in marine environment: Is there an effect of the polymerizable group on the antifouling performance? *Colloids Surf B Biointerfaces* **120**, 118–124 (2014).
- 28 Tsujii, Y., Ohno, K., Yamamoto, S., Goto, A. & Fukuda, T. Structure and properties of high-density polymer brushes prepared by surface-initiated living radical polymerization. *Adv. Polym. Sci.* **63**, 1–45 (2006).
- 29 Kobayashi, M., Terayama, Y., Hosaka, N., Kaido, M., Suzuki, A., Yamada, N. L., Torikai, N., Ishihara, K. & Takahara, A. Friction behavior of high-density poly(2-methacryloyloxyethyl phosphorylcholine) brush in aqueous media. *Soft Matter* **3**, 740–746 (2007).
- 30 Kobayashi, M., Terayama, Y., Yamaguchi, H., Terada, M., Murakami, D., Ishihara, K. & Takahara, A. Wettability and antifouling behavior on the surfaces of superhydrophilic polymer brushes. *Langmuir* **28**, 7212–7222 (2012).
- 31 Kobayashi, M., Terayama, Y., Kikuchi, M. & Takahara, A. Chain dimensions and surface characterization of superhydrophilic polymer brushes with zwitterion side groups. *Soft Matter* **9**, 5138–5148 (2013).
- 32 Kikuchi, M., Terayama, Y., Ishikawa, T., Hoshino, T., Kobayashi, M., Ogawa, H., Masunaga, H., Koike, J., Horigome, M., Ishihara, K. & Takahara, A. Chain dimension of polyampholytes in solution and immobilized brush states. *Polym. J.* **44**, 121–130 (2012).
- 33 Kobayashi, M., Ishihara, K. & Takahara, A. Neutron reflectivity study of the swollen structure of polyzwitterion and polyelectrolyte brushes in aqueous solution. *J. Biomater. Sci. Polym. Ed.* **25**, 1673–1686 (2014).
- 34 Zhulina, E. B. & Rubinstein, M. Ionic strength dependence of polyelectrolyte brush thickness. *Soft Matter* **8**, 9376–9383 (2012).
- 35 Dunlop, I. E., Thomas, R. K., Titmus, S., Osborne, V., Edmondson, S., Huck, W. T. S. & Klein, J. Structure and collapse of a surface-grown strong polyelectrolyte brush on sapphire. *Langmuir* **28**, 3187–3193 (2012).
- 36 Murakami, D., Takenaka, A., Kobayashi, M., Jinnai, H. & Takahara, A. Measurement of the electrostatic interaction between polyelectrolyte brush surfaces by optical tweezers. *Langmuir* **29**, 16093–16097 (2013).
- 37 Kobayashi, M., Tanaka, H., Minn, M., Sugimura, J. & Takahara, A. Interferometry study of aqueous lubrication on the surface of polyelectrolyte brush. *ACS Appl. Mater. Interfaces* **6**, 20365–20371 (2014).
- 38 Terayama, Y., Kikuchi, M., Kobayashi, M. & Takahara, A. Well-defined poly(sulfobetaine) brushes prepared by surface-initiated ATRP using a fluoroalcohol and ionic liquids as the solvents. *Macromolecules* **44**, 104–111 (2011).
- 39 Aldred, N. & Clare, A. S. In: *Functional Surfaces in Biology* (ed. Golb, S. N.) Ch. 2, 43–64 (Springer, Netherlands, 2009).
- 40 Kamino, K. Absence of cross-linking via trans-glutaminase in barnacle cement and redefinition of the cement. *Biofouling* **26**, 755–760 (2010).
- 41 Kamino, K. Molecular design of barnacle cement in comparison with those of mussel and tubeworm. *J. Adhes.* **86**, 96–110 (2010).
- 42 Guo, S., Puniredd, S. R., Jariczewski, D., Lee, S. S. C., Teo, S. L.-M., He, T., Zhu, X. & Vancso, G. J. Barnacle larvae exploring surfaces with variable hydrophilicity: Influence of morphology and adhesion of “Footprint” proteins by AFM. *ACS Appl. Mater. Interfaces* **6**, 13667–13676 (2014).
- 43 Lee, B. P., Messersmith, P. B., Israelachvili, J. N. & Waite, J. H. Mussel-inspired adhesives and coatings. *Annu. Rev. Mater. Res.* **41**, 99–132 (2011).
- 44 Stewart, R. J., Ransom, T. C. & Hladky, V. Natural underwater adhesives. *J. Polym. Sci. B Polym. Phys.* **49**, 757–771 (2011).
- 45 Lu, Q., Hwang, D. S., Liu, Y. & Zeng, H. Molecular interactions of mussel protective coating protein, mcfp-1, from *Mytilus californianus*. *Biomaterials* **33**, 1903–1911 (2012).
- 46 Lee, B. P., Chao, C.-Y., Nunalee, F. N., Motan, E., Shull, K. R. & Messersmith, P. B. Rapid gel formation and adhesion in photocurable and biodegradable block copolymers with high DOPA content. *Macromolecules* **39**, 1740–1748 (2006).
- 47 Nishida, J., Kobayashi, M. & Takahara, A. Light-triggered adhesion of water-soluble polymers with a caged catechol group. *ACS Macro Lett.* **2**, 112–115 (2013).
- 48 Xu, H., Nishida, J., Wu, H., Higaki, Y., Otsuka, H., Ohta, N. & Takahara, A. Structural effects of catechol-containing polystyrene gels based on a dual cross-linking approach. *Soft Matter* **9**, 1967–1974 (2013).
- 49 Schlenoff, J. B. Zwitteration: Coating surfaces with zwitterionic functionality to reduce nonspecific adsorption. *Langmuir* **30**, 9625–9636 (2014).
- 50 Adamczyk, Z. & Weron, P. Application of the DLVO theory for particle deposition problems. *Adv. Colloid Interface Sci.* **83**, 137–226 (1999).
- 51 Marshall, K. C., Stout, R. & Mitchell, R. Mechanism of the initial events in the sorption of marine bacteria to surfaces. *J. Gen. Microbiol.* **68**, 337–348 (1971).
- 52 Morisaki, H., Nagai, S., Ohshima, H., Ikemoto, E. & Kogure, K. The effect of motility and cell-surface polymers on bacterial attachment. *Microbiology* **145**, 2797–2802 (1999).
- 53 Ohshima, H. Electrophoresis of soft particles. *Adv. Colloid Interface Sci.* **62**, 189–235 (1995).

Supplementary Information accompanies the paper on Polymer Journal website (<http://www.nature.com/pj>)